
Maternal and Fetal ^{11}C -Cocaine Uptake and Kinetics Measured In Vivo by Combined PET and MRI in Pregnant Nonhuman Primates

Helene Benveniste, MD, PhD^{1,2}; Joanna S. Fowler, PhD³; William Rooney, PhD³; Yu-Shin Ding, PhD³; Angela L. Baumann, MD^{1,2}; Daryn H. Moller, MD²; Congwu Du, PhD¹; Walter Backus, MD²; Jean Logan, PhD³; Pauline Carter, RN³; Jeremy D. Coplan, MD⁴; Anat Biegon, PhD¹; Leonard Rosenblum, PhD⁴; Bruce Scharf, DVM⁴; John S. Gatley, PhD¹; and Nora D. Volkow, MD⁵

¹Medical Department, Brookhaven National Laboratory, Upton, New York; ²Department of Anesthesiology, State University of New York at Stony Brook, Stony Brook, New York; ³Chemistry Department, Brookhaven National Laboratory, Upton, New York; ⁴Department of Psychiatry, State University of New York Downstate, Brooklyn, New York; and ⁵National Institute on Alcohol Abuse and Alcoholism, National Institutes of Health, Bethesda, Maryland

Cocaine use during pregnancy has been shown to be deleterious to the infant. This may reflect reduction of flow to placenta or effects on the fetal brain. Methods to assess pharmacokinetics of drugs of abuse in vivo would be useful to investigate the mechanisms underlying the fetal adverse effects. We recently reported that combined MRI and PET technology allows the measurement of radioisotope distribution in maternal and fetal organs in pregnant *Macaca radiata*. Here, we evaluate the utility of PET to measure the uptake and distribution of ^{11}C -cocaine in the third-trimester fetus. **Methods:** Six pregnant *M. radiata* weighing 3.8–9.0 kg were anesthetized and MR images were acquired on a 4-T MRI instrument. In all 6 animals, dynamic PET scans were subsequently acquired using 148–259 MBq of ^{11}C -cocaine. Time–activity curves for both maternal and fetal organs were obtained simultaneously with the pregnant animal positioned transverse in the PET scanner. Distribution volume ratios for maternal and fetal brain for ^{11}C -cocaine were calculated. **Results:** Coregistration of PET and MR images allowed identification of fetal organs and brain regions and demonstrated that ^{11}C -cocaine or its labeled metabolites readily cross the placenta and accumulate mainly in fetal liver and to a lesser extent in the brain. Time to reach peak ^{11}C uptake in brain was shorter for the mother than for the fetus. The distribution volume ratios of the maternal striatum were higher than those of the fetus. Placenta was clearly visible on the early time frames and showed more rapid uptake and clearance than other fetal tissues. **Conclusion:** The pregnant *M. radiata* model allows the noninvasive measurement of radioisotope pharmacokinetics in maternal and fetal brain and other organs simultaneously. Although the uptake of radioactivity into the fetal brain after the injection of ^{11}C -cocaine is lower and slower than in the maternal brain, a measurable quantity of ^{11}C -cocaine (or its labeled metabolites) accumulates in the fetal brain at early times after injection. The highest accumulation of ^{11}C occurs in the fetal liver. Rapid

radioisotope accumulation and clearance in the placenta offer potential as an input function for kinetic modeling for future studies of binding site availability.

Key Words: ^{11}C -cocaine; maternal–fetal exchange; PET; MRI; primate

J Nucl Med 2005; 46:312–320

An understanding of how drugs are transferred between mother and fetus during the gestational period is an important medical and health issue that is of relevance to both therapeutic drugs and drugs of abuse. Concerns about ethical and medical safety prohibit most studies of maternal–fetal exchange in humans, and animal models have therefore been developed (1–3). For example, the model of chronically catheterized fetal and maternal sheep has been used in pioneering studies on maternal–fetal exchange of anesthetics and physiologic studies of the maternal–fetal circulation (4,5). Similarly, pregnant rhesus macaques with chronically implanted venous catheters have been used to study maternal and fetal pharmacokinetics of cocaine and other drugs of abuse (6,7).

In all studies discussed above, invasive approaches were used to obtain maternal and fetal drug exchange data and pharmacokinetic profiles. Hartvig et al. were the first to introduce PET as a potential tool to study maternal–fetal exchange noninvasively (8) using ^{11}C -labeled radiotracers. ^{11}C has a 20.4-min half-life and decays by positron emission to produce two 511-keV photons that penetrate the body barrier and can be imaged externally using coincidence detection. They pointed out the difficulties of accessing the fetal compartments without disturbing the normal physiology in the invasive models and suggested the use of noninvasive imaging to study rapid transfer of ^{11}C -labeled drugs from mother to fetus. Although some interpretation of

Received Sep. 14, 2004; revision accepted Dec. 13, 2004.

For correspondence or reprints contact: Helene Benveniste, MD, PhD, Medical Department, Bldg. 490, Brookhaven National Laboratory, 30 Bell Ave., Upton, NY 11793.

E-mail: Benveniste@bnl.gov

pharmacokinetics could be made for ^{11}C -heroin and other compounds with regard to the placenta, it was difficult to identify fetal organs in this study because of lack of spatial resolution on the PET images and thus limited fetal anatomic information (8).

We recently combined whole-body PET and MRI techniques in a study of placental transfer and maternal–fetal anatomic distribution of ^{18}F -FDG in pregnant *Macaca radiata* (9). Compared with previous studies, this study allowed us to more accurately identify fetal body organs of interest, as we had also acquired the anatomic template from the corresponding MR images. However, in our previous study we performed only static whole-body PET scans, which were initiated 35 min after injection of ^{18}F -FDG. Because of the importance of having pharmacokinetic information both for its intrinsic interest and from the standpoint of binding-site quantification, we designed another series of experiments on pregnant *M. radiata* that would provide us with dynamic, pharmacokinetic information as well as better anatomic delineation of the placenta. We chose ^{11}C -cocaine as an example because its distribution and kinetics are well characterized in the baboon and in the human and because of mounting evidence that fetal exposure to cocaine in utero produces a behavioral phenotype in the offspring that is characterized by significant cognitive deficits and a doubling of the rate of developmental delay during the first 2 y of life even when other variables during pregnancy are considered (10).

MATERIALS AND METHODS

Six female bonnet macaques (*M. radiata*) obtained from the Primate Laboratory, Department of Psychiatry, State University of New York (SUNY) Downstate, were used in this study. The experimental protocol was approved by the Institutional Animal Care and Use Committees of Brookhaven National Laboratory and SUNY Downstate. At the SUNY Downstate Primate Laboratory, the bonnet macaques are socially housed in stable groups of 5–8 subjects. Social groups of this species have been housed in the SUNY Downstate laboratory for nearly 4 decades, and health, reproductive patterns, and longevity are well characterized (11).

Five monkeys were judged to be in late third-trimester gestational stage and one in the late second or early third trimester by the veterinarian after a brief physical examination and ultrasound, which was performed at the Primate Laboratory under ketamine anesthesia (8 mg/kg intramuscular injection) (Table 1). The monkeys were transported to Brookhaven National Laboratory 2 wk before the study and were housed according to National Institutes of Health guidelines at the Brookhaven National Laboratory vivarium.

Anesthesia and Physiologic Monitoring for Imaging

In preparation for imaging, the animals were anesthetized with an intramuscular injection of ketamine (10 mg/kg) and glycopyrrolate (0.02 mg/kg) using a squeeze cage. Routine monitors were placed, which included noninvasive blood pressure monitoring, pulse oximetry, body temperature measurement, and electrocardiography. In 3 animals, electroencephalogram monitoring (Bispectral Index [BIS]; Aspect Medical Systems) was also performed

TABLE 1
Subject Demographics and Radiotracers

Subject	Maternal age (y)	Maternal body weight (kg)	Fetal position at time of experiment
BY42	4.1	5.0	Head down
BV37	7.4	9.0	Head down
BY13	4.9	4.5	Head down
BR42	5.5	5.2	Head up
BA22	2.9	4.7	Head down
AA18	2.3	3.8	Head down

during induction of anesthesia and PET. Two intravenous lines were established in the saphenous veins bilaterally. Intravenous hydration was provided using high-molecular-weight hydroxyethyl starch, 6%, in buffered electrolyte dextrose solution, 5–10 mL/kg (Hextend; BioTime, Inc.), administered in 10-mL boluses to a maximum of 20 mL/kg. With careful attention to physiologic parameters, a continuous infusion of propofol (Diprivan, 120 $\mu\text{g}/\text{kg}/\text{min}$; AstraZeneca), and remifentanyl hydrochloride (Ultiva, 0.1 $\mu\text{g}/\text{kg}/\text{min}$; GlaxoSmithKline) was started using a microinfusion pump (model AS50; Baxter). For one animal (BY42), only propofol was administered. Within 1 min of the start of infusion, conditions were met (no lid reflex and BIS < 50) for oral intubation and a 3.5-mm cuffed endotracheal tube was placed and secured. Correct tube placement was confirmed by auscultation and presence of end-tidal CO_2 . Mechanical ventilation was initiated using a volume-controlled ventilator (Inspira; Harvard Apparatus) at a 60%–70% fractional concentration of oxygen in inspired gas. The minute ventilation was adjusted to achieve end-tidal CO_2 values of approximately 30–35 mm Hg. The propofol and remifentanyl infusion was adjusted to maintain the animal at an adequate anesthetic depth (unresponsive to the presence of the endotracheal tube and mechanical ventilation as well as physiologically stable). During the entire procedure, the maternal body temperature was maintained at 36°C–37°C by use of a forced-air warming blanket (Bair Hugger; Arizant Healthcare Inc.). No muscle relaxation was used.

At the conclusion of the imaging experiments, an orogastric tube was quickly placed and the stomach contents emptied; the anesthesia and intravenous lines were discontinued and the animal recovered spontaneous breathing within 2–5 min, was extubated, and was returned to its cage.

MRI

We chose to use MRI and not CT to image fetal and maternal anatomy in these studies, the reason being the well-known superior contrast-to-noise ratio for brain anatomy on MR images, compared with the noise-to-contrast ratio on CT images. All MRI data were acquired on a 4-T instrument (Varian/Siemens) equipped with a high-performance gradient system (Sonata; Siemens, Inc). A radiofrequency transceiver coil with a 27-cm inner diameter was used for all studies. A gating signal generated by the Harvard ventilator was used to synchronize the respiration cycle and the MRI acquisition to avoid maternal respiratory motion artifacts on the MR images. A custom-built mechanical stage was used to secure the animal in the lateral decubitus position in the radiofrequency coil (and later in the PET scanner).

MRI data were collected using a 2-dimensional multislice dual spin-echo sequence; proton density (echo time, 15 ms; repetition

time, 3,000 ms) and T2-weighted (echo time, 50 ms; repetition time, 3,000 ms) MR images were acquired using sixty-five 2-mm slices with a nominal in-plane resolution of 0.63×0.78 mm using a matrix of 512×256 and a total acquisition time of 40 min. The raw data were reconstructed by Fourier transform and displayed as magnitude images. The MR images were reconstructed immediately after the acquisition to ensure adequate image quality for the study. In 2 monkeys, the scans were repeated because of excessive fetal motion (the maternal anesthetics were increased during the repeated scans, with careful attention to hemodynamic parameters).

[N-¹¹C-Methyl]-(-)-Cocaine Synthesis

[N-¹¹C-methyl]-(-)-cocaine was prepared by the reaction of ¹¹C-labeled methyl iodide prepared by a gas phase synthesis system with norcocaine dissolved in 300 μ L of acetonitrile and 200 μ L of methylsulfoxide:diethylformamide (1:4) at 135°C. The labeled cocaine was purified by semipreparative high-performance liquid chromatography (silica gel, Ultrasphere-Si, 10×250 mm; Beckman Inc.) using a solvent mixture consisting of acetonitrile: 0.004 mol/L (NH₄)₂PO₄ (70:30, v/v) and a flow rate of 6 mL/min. The retention time of norcocaine in this system was 10–11 min, and the retention time of ¹¹C-cocaine was 15–16 min. The solvent was evaporated from the fraction containing the labeled cocaine, and the residue was dissolved in 3 mL of isotonic saline for injection. The total synthesis time was 35 min. The radiochemical purity was >98%, and the specific activity was 9.25 GBq/ μ mol at the time of injection.

Dynamic PET Scanning Procedures Using ¹¹C-Cocaine

PET scans were performed on an ECAT EXACT HR+ tomograph (Siemens/CTI) with a 56-cm transaxial and 15.5-cm axial field of view (FOV) surrounded by detector blocks of 4×4 mm bismuth germanate crystals 30 mm long. To obtain the time course of activity in both maternal and fetal brain, both must be in the FOV for the entire study. Because the axial FOV of our CTI HR+ scanner is only 15.5 cm, this requires positioning the animal transverse to the scanner axis such that the animal occupies nearly the entire transverse FOV of 56 cm. As illustrated in Figure 1, we



FIGURE 1. Pregnant bonnet macaque in transverse position within HR+ PET scanner. For dynamic PET studies, pregnant monkey was positioned so that maternal and fetal organs were within same field of view.

changed the positioning of the animals to transverse, instead of the conventional position of cephalad-to-caudal axis transaxial to the center of the PET scanner, to be able to capture maternal and fetal brain time–activity curves in parallel. We performed ¹¹C-cocaine imaging on 6 pregnant animals (Table 1). Emission data were collected using acquisition windows of 350–650 keV for energy and 12 ns for coincidence timing. To maximize sensitivity, we used 3D mode (septa retracted), which gives a spatial resolution at the center of the FOV of 4.6 mm transaxially and 4.2 mm axially (using National Electrical Manufacturers Association NU-2 protocols). We obtained a separate 15-min ⁶⁸Ge transmission scan before injection to correct for attenuation by eliminating emission contamination, and in 2-dimensional mode (septa extended) to minimize acceptance of scattered events.

PET data were processed in a fully quantitative manner using the vendor ECAT software. Random coincidence events were subtracted “online” using a delayed coincidence method. Attenuation correction sinograms were segmented before application to the emission data to reduce statistical noise propagation, and additional corrections for system dead time, detector normalization, and scattered coincidences were performed. The 3D emission sinograms were subsequently reduced to a set of 2-dimensional sinograms using Fourier rebinning and then reconstructed into a 256×256 (transverse) \times 63 (axial) image matrix using the attenuation-weighted ordered-subsets expectation maximization algorithm. Six iterations with 16 subsets were used, and the images were postfiltered with a gaussian kernel of 4 mm in full width at half maximum to control noise. All studies were performed using a dynamic acquisition sequence with the following ¹¹C-cocaine time framing: 4×30 s, 4×60 s, 4×120 s, and 8×300 s.

Image Analysis

Fetal total volume and individual fetal organ volumes were assessed by manually segmenting areas of interest on the interpolated 3D MRI dataset using Amira 3.1 (TGS, Inc.). The PET image analysis comprised multiple processing steps and different software packages. First, all time frames were viewed in a cinematic mode (PMOD biomedical image quantification software, version 2.5; PMOD Technologies) to determine gross movement during the acquisition. Second, all time frames of the dynamic time study were added, and the summed ¹¹C-cocaine PET scan and corresponding 3D MR dataset were displayed side by side as isotropic 3D volumes using Amira 3.1. Corresponding external and internal anatomic landmarks were identified and marked on both datasets using the Landmarkset module (Amira 3.1). The marked MRI dataset was subsequently warped, using a rigid warp algorithm, to the corresponding marked ¹¹C-cocaine 3D summed PET dataset that served as the master template. Third, the warped MRI 3D dataset was imported as the reference template into the fusion module of PMOD. Fetal regions of interest (ROIs)—that is, corpus striatum, cerebellum, heart, lungs, liver, placenta, and the entire uterine content—were outlined directly on the warped MR image overlaid on the corresponding dynamic ¹¹C-cocaine PET dataset. (The cerebellum in the second-trimester fetus could not clearly be identified on the PET images because of a fetal positional change in relation to the corresponding MR images). Early time frames were used to accurately identify the placenta; maternal heart, lungs, and kidneys; and fetal liver. Maternal ROIs (corpus striatum, cerebellum, liver, and heart) were identified directly on the ¹¹C-cocaine PET scan, because the MRI reference template did not include the entire maternal body. The radioactivity concentration

in the ROIs was used to obtain the time–activity curve of regional tissue concentrations. All ROI radioactivity was converted from nCi/cm³ to standardized uptake values (SUVs, calculated as [(ROI activity in nCi/cm³) × (body weight in kg)]/[(total injected dose in nCi) × 1,000]). Time–activity curves for tissue concentration changes within the corpus striatum and cerebellum were used to calculate the distribution volume ratios (DVRs) using the DVR (Logan noninvasive) configuration in the PMod module (PMOD). Figure 2A illustrates the warping step of the multiple software image analysis processes.

RESULTS

Morbidity and Mortality

All *M. radiata* survived the experiments with no adverse events. Five of 6 animals delivered healthy babies that appeared to be full term (full crown of hair). One animal delivered a stillborn fetus 2 d after the experiment, and the fetus was clearly not viable at the time of MRI and PET as indicated by low contrast-to-noise ratio on the T2- and proton-density–weighted images and lack of radiotracer activity in the placenta and uterine cavity. Hemodynamic parameters were stable during the entire scanning processes and could not explain the cause of the fetal death.

Anesthesia and Physiologic Monitoring

The animals remained physiologically stable (O₂ saturation, >98%; end-tidal CO₂, >29 mm Hg; body temperature, 36°C–37°C; heart rate, 80–120 bpm) during the entire experiment. The blood pressure and pulse rate were high (approximately 100/60 mm Hg and 120–140 beats per minute, respectively) during the first 30 min because of the ketamine and the initial stress. During PET, the average (±SD) systolic and diastolic blood pressures were 74 ± 3 mm Hg and 39 ± 2 mm Hg, respectively. All PET studies

were conducted >2.5 h after the initial ketamine injection, ensuring that the effect of ketamine was minimal at the time of PET data acquisition (elimination half-life of ketamine, 2.5 h). No measurable changes in heart rate or blood pressure occurred when the ¹¹C-cocaine tracer dose was administered.

MRI Data Analysis

As shown in Figure 3A, the T2-weighted MR images showed anatomic fetal detail better than did the proton-density–weighted images. For example, the fetal liver and placenta were much better defined by T2 contrast than by proton-density contrast. However, the proton-density–weighted images outlined fetal vessels extremely well, as shown in Figure 3B. In fact, in one of the third-trimester fetuses, the umbilical cord vessels, ductus venosus, and vena cava inferior could be identified (Fig. 3B). In 5 of the pregnant *M. radiata*, the fetus was in vertex presentation (the fetal head was the presenting part), whereas 1 fetus was in breech position (head was not the presenting part).

Maternal respiratory gating during the MRI data acquisition significantly reduced overall image-motion artifacts. In the third-trimester fetuses, gross fetal motion such as a change in position of the fetal head/extremities or whole-body rotation (e.g., from vertex to breech) were not evident on the PET images although the MR images were acquired 1–2 h before the PET images. However, the PET images of the second-trimester fetus clearly revealed that the fetus had moved (more transverse position), probably because of increased maternal bladder filling and overall greater mobility of the smaller fetus.

T2- and proton-density–weighted MR images of the third-trimester fetal brains revealed limited neuroanatomic detail

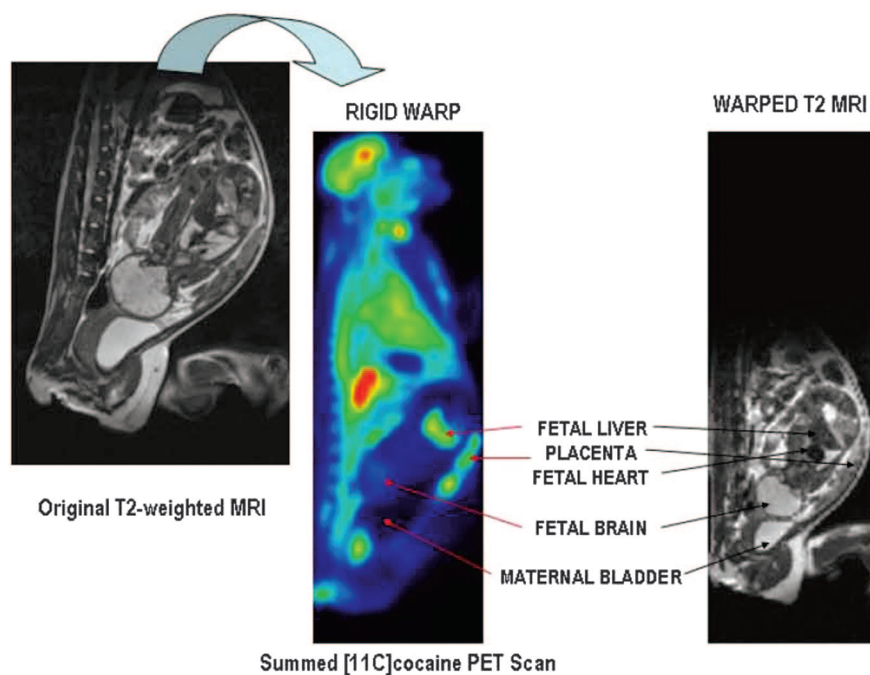


FIGURE 2. (Left) T2-weighted MR image of third-trimester pregnant *M. radiata*. Spatial resolution of original MR image is 0.78 × 0.625 × 2 mm. (Middle) ¹¹C-Cocaine PET image with all time frames summed, color coded using Amira 3.1. (Right) T2-to-summed PET warped T2 image. Spatial resolution of warped MR image is 2.57 × 2.57 × 2.42 mm. Placenta, maternal bladder, and fetal organs of interest are indicated. Maternal bladder (dark structure) appears larger on summed PET image because of filling of bladder during the approximately 2-h PET procedure.

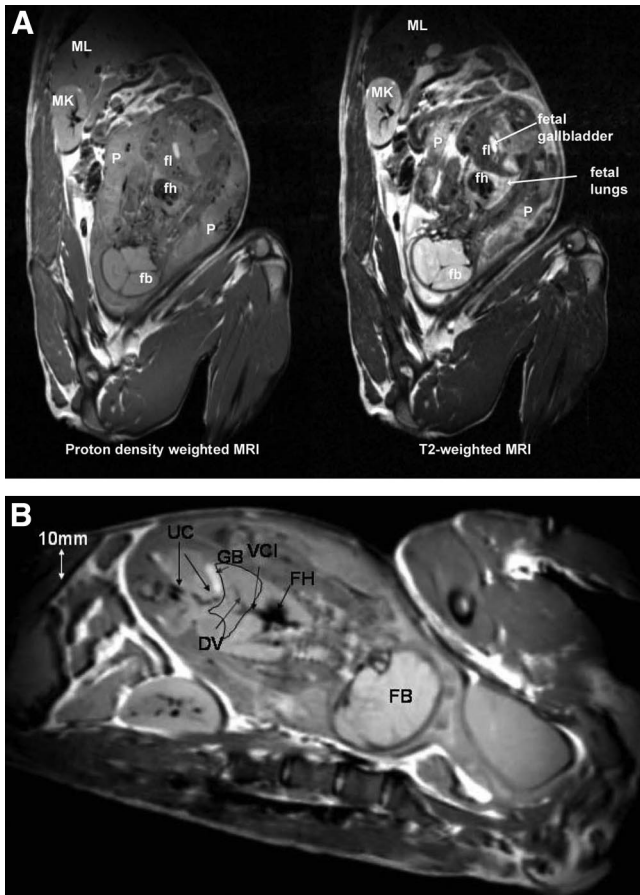


FIGURE 3. (A) Proton density-weighted (left) and corresponding T2-weighted (right) MR images from third-trimester pregnant *M. radiata*. fb = fetal brain; fh = fetal heart; fl = fetal liver; MK = maternal kidney; ML = maternal liver; P = placenta. (B) Proton density-weighted MR image from third-trimester pregnant *M. radiata* illustrating superior visualization of fetal vessels. Fetal liver has been outlined as anatomic landmark. DV = ductus venosus; FB = fetal brain; FH = fetal heart; GB = gallbladder; UC = umbilical cord; VCI = vena cava inferior. Diameter of DV is approximately 1–2 mm.

because of lack of myelination and thus lower contrast-to-noise ratio in the images. However, major brain structures such as forebrain, ventricles, corpus callosum, midbrain, and cerebellum could be identified (Fig. 4). The volumes of the fetus and fetal body organs (heart, lungs, liver, and brain) in the 5 pregnant *M. radiata* with live fetuses are listed in Table 2. The data seemed to indicate that the fetal liver rapidly enlarged near term and that the brain volume was relatively constant from the middle of the third trimester until term. Further, a 3- to 4-fold difference was seen between heart volume and liver volume in third-trimester fetuses. Interestingly, the biggest mother had the biggest baby brain by far.

¹¹C-Cocaine PET Data Analysis

Figure 5 shows a time series of ¹¹C-cocaine PET dynamic scans from a third-trimester pregnant animal, overlaid on their corresponding warped T2-weighted MR images; the first, second, fifth, 11th, and 16th time frames are shown at

the anatomic level of the fetal brain, liver, and heart. The maternal heart, liver, and brain are also in the field of view. In contrast to other fetal organs, the placental vessels, maternal heart, maternal kidneys, and fetal liver were easily identified on the early time frames, as can be seen in Figure 5.

The corresponding body organ time-activity curves of the 4 third-trimester pregnant *M. radiata* are shown in Figure 6A and demonstrated high ¹¹C uptake in maternal heart, lungs, and kidneys. The times to peak ¹¹C uptake for maternal heart, lungs, and kidneys were 7.6 (SD, 1.7), 11.0 (SD, 6.3), and 9.7 (SD, 3.6), respectively. Further, in the third-trimester animals the time-activity profile of ¹¹C uptake in the maternal liver and brain demonstrated slower uptake and no clear peak activity. Interestingly, the second-trimester pregnant animal anesthetized with only propofol demonstrated significantly higher ¹¹C peak uptake in the maternal liver than did the animals anesthetized with both propofol and remifentanyl (second-trimester peak SUV of 4.2 in maternal liver, vs. 1.94 ± 0.26 in the 4 third-trimester pregnant animals at 3.5 min after injection). The maternal corpus striatum ¹¹C uptake was higher than the maternal cerebellum uptake after 5–6 min of tracer circulation time. The ¹¹C uptake in the uterine cavity displayed a temporal profile similar to that of the maternal brain and liver but with significantly less activity.

The average uptake and kinetics of ¹¹C-cocaine and labeled metabolites in third-trimester fetal organs and placenta are shown in Figure 6B. The distribution pattern of ¹¹C-cocaine uptake in the fetus during the dynamic PET study was very different from that in the mother. For example, in the fetus the total ¹¹C uptake in the liver was higher than that in any other fetal organ, whereas in the mother liver uptake represented a much smaller total uptake, compared with uptake in the heart and kidneys. The peak ¹¹C concentration for the fetal liver had an SUV of 2.52 (SD, 0.22) and occurred at 5.5 min after administration of the tracer. Half of the peak activity in the fetal liver remained at 20 min. Additionally, in contrast to the fetal lungs, which did not display peak activity but instead a slow, plateaulike uptake over the 51-min circulation time,

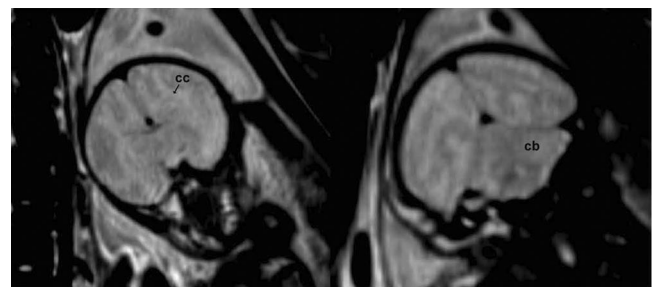


FIGURE 4. T2-weighted MR images of fetus BY13. Overall contrast-to-noise ratio is limited, but gray matter and white matter areas can be appreciated, as well as gross neuroanatomic structures such as corpus callosum (cc), cortex, midbrain, and cerebellum (cb).

TABLE 2
Fetal Volumes in Subjects with Live Fetuses

Subject	Gestation (d) at time of experiment*	Total fetal volume (cm ³)	Fetal heart	Fetal lungs	Fetal liver	Fetal brain
BY42	92/170, second	69.8	0.3	—	1.6	15.9
BR42	122/170, third	154.1	1.5	5.0	6.0	32.4
BY13	133/170, third	198	1.8	5.8	6	37.0
BA22	147/170, third	156.3	3.2	8.1	11.6	35.2
BV37	155/170, third	282.5	3.0	6.9	12.1	49.6

*Gestational age at time of experiment was estimated by assuming 170 d of gestation and subtracting number of days from day of experiment to known time of delivery.

¹¹C uptake in the maternal lungs was rapid and the radioactivity was not retained. Finally, we observed no ¹¹C uptake or retention in the fetal heart, in contrast to the observations for the maternal heart (Fig. 6A). The fetal striatum and cerebellum demonstrated a slow rise over the first 15–20 min of circulation time, with the corpus striatum ¹¹C uptake being consistently higher than ¹¹C uptake in fetal cerebellum. Uptake of ¹¹C in the placenta reached a maximum 1 min after injection of the tracer, and clearance (half-peak activity was reached at 7–10 min) was similar to that of maternal heart (Fig. 6B).

Table 3 shows the ratio of the ¹¹C distribution volume in the corpus striatum and the distribution volume in the cer-

ebellum (DVR) for both the mother and the fetus, calculated using the noninvasive Logan plot approach (12). The maternal DVRs were statistically significantly ($P = 0.0016$) higher (11%–22%) than those of the fetus.

DISCUSSION

The major findings of our study are, first, that the uptake and kinetics of ¹¹C-cocaine and its derived ¹¹C metabolites can be measured simultaneously and noninvasively in maternal and fetal body organs in third-trimester pregnant *M. radiata* by combining PET and MRI; second, that maternal and fetal organ distributions of ¹¹C are significantly different; third, that the organ of highest accumulation of ¹¹C in the fetus is the liver; fourth, that the fetal brain accumulates and clears ¹¹C to a lesser degree and more slowly than does the maternal brain, and accumulation is in a region probably corresponding to the striatum; fifth, that the placenta is visible on the early frames of the PET image; and sixth, that the distribution volume of the corpus striatum to that of the cerebellum can be calculated using the noninvasive Logan plot approach in both the mother and the third-trimester fetal brain under tracer conditions in which cocaine has no pharmacologic effect on the maternal–fetal unit.

The distribution pattern and kinetics of ¹¹C-cocaine in the whole body of the maternal *M. radiata* were similar to those previously described for whole-body PET scans of humans (13), with fast uptake and clearance in the heart, kidneys, and lungs and slower uptake in the liver and brain. The cardiac peak activity and clearance of ¹¹C-cocaine was faster in maternal pregnant *M. radiata* than in humans (peak activity within 30 s and half-peak activity within 1 min, compared with peak activity at 2–3 min in humans (13)), most likely because of the effect of anesthesia, pregnancy, and species differences in cardiac output. In the fetus, the anatomic ¹¹C-cocaine uptake distribution pattern was very different from that in the mother. For example, in the fetus total ¹¹C uptake was higher in the liver than in the heart and lungs. Further, ¹¹C uptake did not reach a peak in the fetal lungs and heart, which instead displayed a slow rate of uptake including retention of low levels of ¹¹C activity over the entire circulation time. The ¹¹C distribution uptake dif-

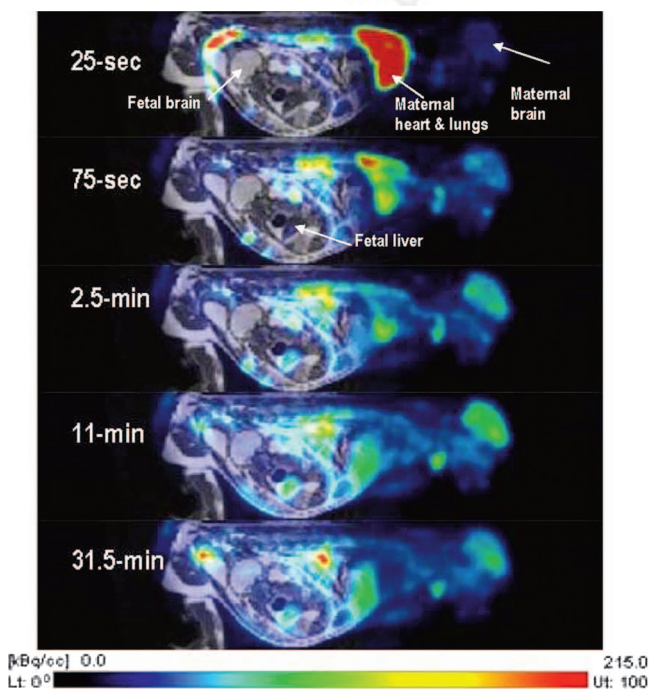


FIGURE 5. Time series of ¹¹C-cocaine PET scans from third-trimester pregnant *M. radiata*. Each PET frame is coregistered to corresponding MR image. Early PET frames (25 s, 75 s, and 2.5 min) clearly show early ¹¹C uptake in placental vessels, maternal heart, lungs, and kidneys. Later time frames demonstrate uptake in fetal liver.

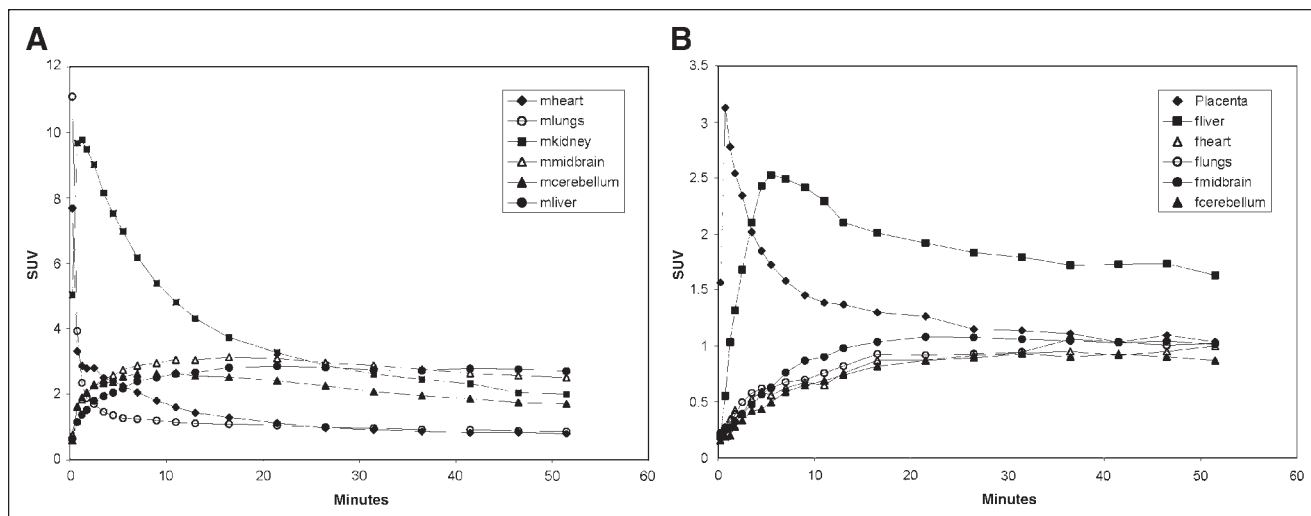


FIGURE 6. (A) Average ($n = 4$) time-activity curves of ^{11}C uptake in maternal organs, including uterine cavity, of third-trimester *M. radiata*. Peak uptake occurred 30 s after injection in heart and lungs and at 1–2 min in kidneys; half activity remained in kidneys at 15 min, in contrast to rapid (<3 min) clearance in maternal heart. (B) Average time-activity curves of ^{11}C -cocaine in placenta, fetal heart, fetal liver, fetal striatum, and fetal cerebellum. Values represent averages for 4 third-trimester fetuses. Placenta and fetal liver have high peak uptake, which contrasts with slower uptake and clearance observed in other fetal organs. The letters *m* and *f* prefixed to name of organ indicate *maternal* and *fetal*, respectively.

ferences between mother and fetus were most apparent in the early time frames and were clearly a consequence of the unique fetal circulation. This study also showed high uptake of ^{11}C -cocaine in the placenta—a relevant finding because cocaine has been shown to cause vasoconstriction of placental blood vessels. Thus, the significant uptake in placenta suggests that this may be one of the mechanisms underlying the deleterious effects of cocaine exposure during pregnancy (14,15). A previous study of pregnant rats examined the tissue distribution of cocaine and metabolites 30 min after a subcutaneous cocaine injection of 30 mg/kg and also documented a high cocaine concentration in the placenta and the fetal liver (16).

The high accumulation of ^{11}C in the fetal liver is expected because blood from the placenta passes via the umbilical vein to the fetal liver, where 30%–70% is shunted via the ductus venosus, a narrow vessel positioned within the liver

parenchyma that directly connects the umbilical vein and the vena cava inferior (5). Because of limited spatial resolution in the PET images (volume-averaging effects), we could not separate the ductus venosus from the hepatic circulation. Consequently, the high (and peak) ^{11}C uptake in the fetal liver clearly reflects collective flow via the ductus venosus, vena cava inferior, and hepatic circulation. Similarly, in the fetal heart we observed a relatively fast ^{11}C uptake over the first 4.5 min followed by a slower uptake, which also can be attributed to volume-averaging effects in the PET images, as the fetal heart is situated near the fetal liver and is a much smaller organ as documented by the MR images (Table 2).

The ^{11}C -cocaine brain kinetics directly measured in the maternal-fetal unit in this study largely agree with previous pharmacokinetic data on cocaine obtained by nonimaging methods. For example, in pregnant rhesus monkeys the maximum cocaine plasma concentration in the maternal jugular vein and fetal internal jugular vein after a single intravenous dose of cocaine to the mother is reached within 1–2 min (7). Further, in rhesus monkeys (7) and ewes (17) the maximal maternal plasma levels of cocaine were 5–10 times higher than the peak levels in the fetus. In the present study we compared the ^{11}C bolus in the maternal and fetal heart as an estimate of the plasma ratios. The ratio of ^{11}C uptake at its peak in maternal heart to ^{11}C uptake at 4.5 min in fetal heart was approximately 13 (SUVs of 7.67 and 0.58, respectively). In a now-classic study by Woods et al., maternal and fetal serum cocaine levels were measured in pregnant ewes after a single injection of cocaine to the mother (3). The data demonstrated that fetal cocaine levels declined rapidly after 4–5 min, remained at low levels at 30

TABLE 3
 ^{11}C -Cocaine Binding in Maternal and Fetal Striatum

Subject	DVR		Mother-to-fetus ratio
	Mother	Fetus	
BV37 (MKY013)	1.38	1.22	1.13
BY13 (MKY015)	1.27	1.14	1.11
BA22 (MKY024)	1.61	1.31	1.22
BR42 (MKY022)	1.17	1.03	1.13
AA18 (MKY026)	1.34	—	—
Average \pm SD	1.35 \pm 0.16	1.17 \pm 0.13*	

* $P < 0.0016$.

min, and became undetectable by 60 min, illustrating the ability of the fetus to metabolize cocaine or redistribute cocaine to other fetal organs (3). In this study, ^{11}C uptake in the fetal heart and other fetal organs did not clear completely after 51 min because ^{11}C -cocaine and its derived ^{11}C -metabolites such as benzoylecgonine cannot be separated without obtaining blood samples from the fetal circulation.

This noninvasive PET study with ^{11}C -cocaine did not provide direct information on the chemical form of ^{11}C that is delivered to the fetal organs or the chemical form of the ^{11}C that is present in the brain and the liver. However, the fetal metabolism of cocaine has been characterized by several investigators. In the adult organism, cocaine is known to be broken down initially into 3 major metabolites by means of cleavage of the benzoyl ester by serum and hepatic esterases to produce ecgonine methyl ester, cleavage of the methyl ester by enzymatic or spontaneous hydrolysis yielding benzoylecgonine, and *N*-demethylation by cytochrome P-450 enzymes to produce norcocaine (18). Cocaine and lipophilic metabolites (norcocaine) pass readily across the placenta (3). However, the fetus is known to be capable of metabolizing cocaine to benzoylecgonine, and the pharmacokinetics of benzoylecgonine have been documented in fetal sheep, rats, and rhesus monkeys. In fact, compared with cocaine, benzoylecgonine is relatively hydrophilic, and the major source of fetal benzoylecgonine therefore most likely stems from the fetus's own metabolic breakdown of cocaine and not from maternal transfer of this compound. Small amounts of norcocaine have been found in the amniotic fluid of both humans and sheep, indicating that the fetus might be capable of producing this metabolite.

In this PET study, norcocaine produced in the mother would not contribute to the ^{11}C uptake seen in the fetus because the *N*-demethylation of ^{11}C -labeled cocaine leads to unlabeled norcocaine, which would not be detected (19). Therefore, since norcocaine is the only metabolite of cocaine that is behaviorally active and norcocaine derived from [*N*- ^{11}C -methyl]cocaine would not be labeled, it is highly probable that the ^{11}C in both maternal and fetal brain over this short experimental period is cocaine itself (20). We previously compared the distribution and kinetics of cocaine labeled in both the *N*- and the *O*-methyl positions, as well as labeled benzoylecgonine, in the baboon to demonstrate that norcocaine does not contribute any activity to the PET image of the baboon brain and that benzoylecgonine does not cross the blood-brain barrier (20). The current investigation of the distribution of cocaine and its labeled metabolites could be expanded to include the use of [*O*- ^{11}C -methyl]cocaine and ^{11}C -benzoylecgonine to tease apart the contribution of cocaine and its metabolites in the fetal compartment. An additional consideration would be differences in protein binding of cocaine between the maternal plasma and the fetal compartment. However, it is known

that cocaine, as a weak base, is only 8%–10% protein bound in human plasma, suggesting that most administered cocaine is available to equilibrate with the fetal circulation (21).

The uptake and clearance of ^{11}C -cocaine in the maternal brain were similar to those described for brains of humans and baboons (19), with peak uptake between 4 and 10 min and slower clearance in the striatum than in the cerebellum. The third-trimester fetal brains displayed the same temporal ^{11}C uptake and clearance patterns in the striatum and the cerebellum. In addition, because cocaine binds to the dopamine transporter, radiotracer studies with ^{11}C -cocaine provide the potential for measurement of dopamine transporter availability in the fetal brain during ontogeny. We determined the DVR, which is equal to $B_{\text{max}}/k_d + 1$ (where B_{max} is maximum binding density and k_d is binding affinity), using the method developed by Logan et al. (12) for ^{11}C -cocaine that uses a reference region (the cerebellum) that has no dopamine transporter binding. The DVR values calculated for the maternal *M. radiata* brains averaged 1.35, which is somewhat lower than values reported for humans and baboons—1.62 (12) and 1.6 (22), respectively. Though small, uptake in fetal brain was still significant. This is important because studies have shown that dopamine transporters, which are the main targets for cocaine effects, are functionally active during this stage of development. Thus, fetal dopamine transporter blockade by cocaine would result in enhanced dopaminergic stimulation. Indeed, studies in dopamine transporter knockout animals have shown decreased growth as a result of enhanced dopaminergic tone in hypothalamus, which leads to inhibition of hypothalamic cells that secrete growth hormone (23).

CONCLUSION

In this study we demonstrate the feasibility of using PET and MRI to directly and simultaneously measure the pharmacokinetics of ^{11}C -cocaine and its labeled metabolites in the maternal and fetal organs. Although uptake of radioactivity after injection of ^{11}C -cocaine is lower and slower in the fetal brain than in the maternal brain, a measurable quantity of ^{11}C -cocaine accumulates in the fetal brain early after injection. However, the highest accumulation of ^{11}C occurs in the fetal liver. Rapid radioisotope accumulation and clearance in the placenta offer potential as an input function for kinetic modeling for future studies of binding site availability. There is mounting evidence that fetal exposure to cocaine in utero produces a behavioral phenotype in the offspring that is characterized by significant cognitive deficits and a doubling of the rate of developmental delay during the first 2 y even when other variables during pregnancy are considered. Thus, the data that we present show the ability of PET to directly measure the accumulation of cocaine or its labeled metabolites simultaneously in maternal and fetal organs.

ACKNOWLEDGMENTS

This study was supported by funds from the Office of Biological and Environmental Research, Office of Science, Department of Energy, and by National Institute on Drug Abuse grant 1R21DA0015545.

REFERENCES

1. Kaiser HH, Cummings JN. Plasma electrolytes of the pregnant ewe and fetal lamb. *Am J Physiol.* 1958;193:627–633.
2. Lee CC, Chiang CN. Maternal–fetal transfer of abused substances: pharmacokinetic and pharmacodynamic data. *NIDA Res Monogr.* 1985;60:110–147.
3. Woods JR Jr, Plessinger MA, Scott K, Miller RL. Prenatal cocaine exposure to the fetus: a sheep model for cardiovascular evaluation. *Ann N Y Acad Sci.* 1989;562:267–279.
4. Morishima HO, Heymann MA, Rudolph AM, Barrett CT, James LS. Transfer of lidocaine across the sheep placenta to the fetus. *Am J Obstet Gynecol.* 1975;122:581–588.
5. Rudolph AM, Heymann MA. The circulation of the fetus in utero. *Circ Res.* 1967;21:163–184.
6. Suzuki K, Horiguchi T, Comas-Urrutia A, Mueller-Heubach E, Morishima HO, Adamsons K. Placental transfer and distribution of nicotine in the pregnant rhesus monkey. *Am J Obstet Gynecol.* 1973;119:253–262.
7. Zhou M, Song ZM, Lidow MS. Pharmacokinetics of cocaine in maternal and fetal rhesus monkeys at mid-gestation. *J Pharmacol Exp Ther.* 2001;297:556–562.
8. Hartvig P, Lindberg BS, Lilja A, Lundqvist H, Langstrom B, Rane A. Positron emission tomography in studies on fetomaternal disposition of opioids. *Dev Pharmacol Ther.* 1989;12:74–80.
9. Benveniste H, Fowler JS, Rooney WD, et al. Maternal–fetal in vivo imaging: a combined PET and MRI study. *J Nucl Med.* 2003;44:1522–1530.
10. Singer LT, Arendt R, Minnes S, et al. Cognitive and motor outcomes of cocaine-exposed infants. *JAMA.* 2002;287:1952–1960.
11. Rosenblum LA, Smiley J. Weight gain in bonnet and pigtail macaques. *J Med Primatol.* 1980;9:247–253.
12. Logan J, Fowler JS, Volkow N, Wang GJ, Ding, Y-S, Alexoff DA. Distribution volume ratios without blood sampling from graphical analysis of PET data. *J Cereb Blood Flow Metab.* 1996;16:834–840.
13. Volkow N, Fowler JS, Wolf AP, et al. Distribution and kinetics of carbon-11-cocaine in the human body measured with PET. *J Nucl Med.* 1992;33:521–525.
14. Dow-Edwards D. Developmental toxicity of cocaine: mechanisms of action. In: Lewis M, Bendersky M, eds. *Mothers, Babies, and Cocaine: The Role of Toxins in Development.* Hillsdale, NJ: Lawrence Erlbaum Associates; 1995:5–17.
15. Patel TG, Laungani RG, Grose EA, Dow-Edwards D. Cocaine decreases utero-placental blood flow in the rat. *Neurotoxicol Teratol.* 1999;21:559–565.
16. Lindsay Devane C, Simpkins JW, Miller RL, Braun SB. Tissue distribution of cocaine in the pregnant rat. *Life Sci.* 1989;45:1271–1276.
17. DeVane CL, Burchfield DJ, Abrams RM, Miller RL, Braun SB. Disposition of cocaine in pregnant sheep: I. Pharmacokinetics. *Dev Pharmacol Ther.* 1991;16:123–129.
18. Shuster L. Pharmacokinetics, metabolism, and disposition of cocaine. In: Lakoski JM, Galloway MP, White FJ, eds. *Cocaine: Pharmacology, Physiology, and Clinical Strategies.* Boca Raton, FL: CRC Press; 1992:1–14.
19. Fowler JS, Volkow N, Wolf AP, et al. Mapping cocaine binding sites in human and baboon brain in vivo. *Synapse.* 1989;4:371–377.
20. Gatley SJ, Yu DW, Fowler JS, et al. Studies with differentially labeled [¹¹C]cocaine, [¹¹C]benzoylecgonine, and [¹¹C]- and 4'-[¹⁸F]fluorococaine to probe the extent to which [¹¹C]cocaine metabolites contribute to PET images of the baboon brain. *J Neurochem.* 1994;62:1154–1162.
21. Pastrakuljic A, Derewlany LO, Koren G. Maternal cocaine use and cigarette smoking in pregnancy in relation to amino acid transport and fetal growth. *Placenta.* 1999;20:499–512.
22. Fowler JS, Volkow N, Logan J, et al. Measuring dopamine transporter occupancy by cocaine in vivo: radiotracer considerations. *Synapse.* 1998;28:111–116.
23. Bosse R, Fumagalli F, Jaber M, et al. Anterior pituitary hypoplasia and dwarfism in mice lacking the dopamine transporter. *Neuron.* 1997;19:127–138.

